



This is the author's version of a work that was accepted for publication in the following source:

Fallon, J. B., S. Irving, S. S. Pannu, A. C. Tooker, A. K. Wise, R. K. Shepherd, and D. R. Irvine. 2016. Second spatial derivative analysis of cortical surface potentials recorded in cat primary auditory cortex using thin film surface arrays: Comparisons with multi-unit data. *Journal of Neuroscience Methods*. **267**: 14-20.

**Notice:** Changes introduced as a result of publishing processes such as copy-editing and formatting may not be reflected in this document. For a definitive version of this work, please refer to the published source.

The final publication is available at:

<http://www.sciencedirect.com/science/article/pii/S0165027016300425>

Copyright of this article belongs to: © 2016 Elsevier. B.V.

# Journal: Neuroscience Methods

## Type: Research Article

### Title

Second spatial derivative analysis of cortical surface potentials recorded in cat primary auditory cortex using thin film surface arrays: comparisons with multi-unit data

### Authors

James B. Fallon<sup>a,b,c</sup>, Sam Irving<sup>a</sup>, Satinderpall S. Pannu<sup>d</sup>, Angela C. Tooker<sup>d</sup>,  
Andrew K. Wise<sup>a,b,c</sup>, Robert K. Shepherd<sup>a,c</sup> and Dexter R. F. Irvine<sup>a</sup>

- a. Bionics Institute, Melbourne, Victoria, Australia.
- b. Department of Otolaryngology, University of Melbourne, Melbourne, Victoria, Australia.
- c. Medical Bionics Department, University of Melbourne, Melbourne, Victoria, Australia.
- d. Lawrence Livermore National Laboratory, Livermore, CA.

### Corresponding Author

Dr. James Fallon  
Bionics Institute  
384-388 Albert Street  
East Melbourne, Victoria, Australia, 3002  
Ph: +61 3 9667 7576  
Fax: +61 3 9667 7518  
Email: [jfallon@bionicsinstitute.org](mailto:jfallon@bionicsinstitute.org)

# Abstract

## 1 Background

2 Current source density analysis of recordings from penetrating electrode arrays has  
3 traditionally been used to examine the layer-specific cortical activation and plastic changes  
4 associated with changed afferent input. We report on a related analysis, the second spatial  
5 derivative (SSD) of surface local field potentials (LFPs) recorded using custom designed  
6 thin-film polyimide substrate arrays.

## 7 Results

8 SSD analysis of tone-evoked LFPs generated from the auditory cortex under the recording  
9 array demonstrated a stereotypical single local minimum, often flanked by maxima on both  
10 the caudal and rostral sides. In contrast, tone-pips at frequencies not represented in the region  
11 under the array, but known (on the basis of normal tonotopic organization) to be represented  
12 caudal to the recording array, had a more complex pattern of many sources and sinks.

## 13 Comparison with Existing Methods

14 Compared to traditional analysis of LFPs, SSD analysis produced a tonotopic map that was  
15 more similar to that obtained with multi-unit recordings in a normal-hearing animal.  
16 Additionally, the statistically significant decrease in the number of acoustically responsive  
17 cortical locations in partially deafened cats following 6 months of cochlear implant use  
18 compared to unstimulated cases observed with multi-unit data ( $p = 0.04$ ) was also observed  
19 with SSD analysis ( $p = 0.02$ ), but was not apparent using traditional analysis of LFPs ( $p =$   
20  $0.6$ ).

## 21 Conclusions

22 SSD analysis of surface LFPs from the thin-film array provides a rapid and robust method for  
23 examining the spatial distribution of cortical activity with improved spatial resolution  
24 compared to more traditional LFP recordings.

## **Keywords**

Local field potential; cochlear implant; cortical plasticity; neural prosthesis, sensorineural hearing loss

## **Abbreviations**

ABR	Auditory brainstem response
AI	Primary auditory cortex
ICES	Intra-cochlear electrical stimulation
SEM	Standard error of the mean

## **Highlights**

- 25 A conformable 2-dimension thin-file electrode array is described.
- 26 A method for improved spatial resolution of local field potentials is described.
- 27 Results obtained with the new method are in agreement with multi-unit data
- 28

## 29 **1. Introduction**

30 Current source density (CSD) analysis has been applied to a wide range of neocortical  
31 and other brain structures for over 50 years (Mitzdorf, 1985), and was first used to analyse  
32 recordings from auditory cortex by Müller-Preuss & Mitzdorf (1984). More recently, CSD  
33 analysis has been used in a number of studies investigating the plastic changes that occur in  
34 the auditory cortex as a result of long-term profound deafness and/or chronic intracochlear  
35 electrical stimulation (Klinke et al., 1999; Kral et al., 2005; Middlebrooks, 2008; Schroeder et  
36 al., 2001).

37 By taking the second spatial derivative (SSD) of a series of local field potentials  
38 (LFPs) generated by the superposition of synaptic events (Cottaris & Elfar, 2009), CSD  
39 analysis allows identification of the laminar sources of currents, based on a characteristic  
40 pattern of current sources and sinks. CSD analysis of cortical activity presumes the LFPs are  
41 dominated by signals from within a single cortical column (Mitzdorf, 1985), and changes that  
42 occur in parameters encoded across multiple cortical columns, such as tonotopic  
43 organization, consequently cannot be investigated with CSD. However, surface LFPs are well  
44 suited to studying these phenomena. They were used in the first demonstrations of the  
45 tonotopic organization of primary auditory cortex (AI) (Woolsey & Walzl, 1942), and have  
46 been used to investigate the propagation of ‘travelling’ waves of activity across the cortex  
47 (Kral et al., 2009). Such studies have typically utilized sequential recordings from small (1  
48 mm in diameter) silver or platinum-ball macroelectrodes, although they can also utilize  
49 microelectrode recordings from the cortical surface (e.g. Kral et al., 2009) or the middle  
50 cortical layers (e.g. Norena & Eggermont, 2002). The need to average responses to multiple  
51 presentations of the same stimuli to extract the small (10 – 100  $\mu$ V) LFP from background  
52 activity, and to move the electrode to successive recording sites, makes these experiments  
53 extremely time-consuming. When recordings are made with macroelectrodes, the size of the  
54 LFP can also be influenced by the variable contact of the electrode with the cortical surface

55 over the duration of the recordings. A final issue with standard LFP recording is that LFPs  
56 are a mixture of locally generated potentials and potentials volume conducted from sites up to  
57 1 cm away (Eggermont et al., 2011; Gaucher et al., 2012; Kajikawa & Schroeder, 2011;  
58 Norena & Eggermont, 2002).

59 The present study describes a method for simultaneous recording of LFPs from a  
60 large number of surface recording sites, and a method of analyzing those potentials derived  
61 from CSD analysis. The method utilizes a custom designed thin-film polyimide substrate  
62 electrode array that was developed to be flexible enough to follow the undulating surface of  
63 the primary auditory cortex (AI) in the cat, and allow simultaneous recordings at 32 sites.  
64 Analysis of the data by taking the SSD of the LFPs across the major caudal-rostral tonotopic  
65 axis of the cat AI effectively ‘sharpens’ the LFP recordings to allow a more detailed analysis  
66 of the underlying activity. These procedures were validated by comparing the tonotopic  
67 organization of AI as determined by standard LFP analysis and SSD analysis to that obtained  
68 with multi-unit (MU) recordings in a normal-hearing cat. Additionally, the responsiveness of  
69 the cortex in two groups of partially deafened cats was assessed, revealing a difference in the  
70 acoustic responsiveness of AI in cats that had received chronic intracochlear electrical  
71 stimulation compared to partially deafened, unstimulated controls. This difference, which  
72 was evident in the MU data and was also in accord with previously reported MU data (Fallon  
73 et al., 2009b), was not evident using the standard simpler analysis of the LFPs.

## 74 **2. Materials and Methods**

### 75 *2.1. Recording Electrode Arrays*

76 Details of the fabrication of these types of arrays have been reported previously  
77 (Tooker et al., 2012), and will only be summarized here. The electrode arrays were fabricated  
78 using multiple layers of polyimide and metal. The fabrication process began by depositing the  
79 first layer of polyimide. A first layer of trace metal (gold) was deposited and patterned,  
80 followed by a second layer of polyimide. Interconnection vias were etched into this second

81 layer of polyimide using oxygen plasma. A second layer of trace metal (gold) was then  
82 deposited and patterned. The electrode metal (platinum) was next deposited and patterned. A  
83 final layer of polyimide was deposited and openings for the electrodes were etched using  
84 oxygen plasma.

85         The novel array geometry described in this study was specifically designed to follow  
86 the undulating surface of AI in the cat by utilizing 8 separate fingers, each with 4 electrodes,  
87 for a total of 32 electrodes. The electrodes were 200 $\mu$ m in diameter, with 800 $\mu$ m center-to-  
88 center spacing. The resulting array allowed coverage of the majority of the surface accessible  
89 portion of the cat AI (Figure 2A). Surface tension attracted the array to the cortical surface  
90 and the flexible fingers follow the contours of the cortex ensuring all electrodes made good  
91 electrical contact with the cortical surface.

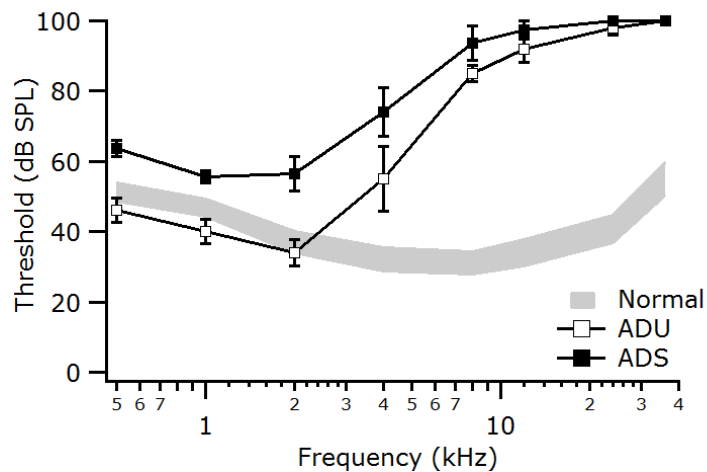
## 92 *2.2. Experimental subjects*

93         Fourteen healthy adult cats with otoscopically normal tympanic membranes and  
94 normal hearing were used in the present study. Hearing status was determined using auditory  
95 brainstem response (ABR) recordings using standard procedures (Irving et al., 2014), with  
96 normal hearing defined as a click-ABR threshold < 32 dB peak equivalent sound pressure  
97 level (SPL). All procedures were in accordance with Australian Code of Practice for the Care  
98 and Use of Animals for Scientific Purposes and with the Guidelines laid down by the  
99 National Institutes of Health in the US regarding the care and use of animals for experimental  
100 procedures, and were approved by the Royal Victorian Eye and Ear Hospital Animal  
101 Research and Ethics Committee.

## 102 *2.3. Deafening procedure*

103         Thirteen cats were administered a daily subcutaneous (s.c.) injection of kanamycin  
104 sulfate (200 mg/kg) for 17 days (Irving et al., 2014), which preferentially damages the high-  
105 frequency basal region of the cochlea. Tone-evoked ABRs were used to determine the degree

106 of hearing loss achieved. Additional daily kanamycin injections were continued until a  
 107 satisfactory high-frequency hearing loss (>60 dB HL at frequencies >8 kHz) had been  
 108 achieved. Mean ABR audiograms for the two partially deafened groups, along with data for a  
 109 large sample (n = 40 ears) of normal-hearing cats, are shown in Figure 1. Thresholds are  
 110 similar to normal for frequencies below 2 kHz, but increase progressively up to 10 kHz, and  
 111 at higher frequencies are at or above our maximum intensity of 100 dB SPL



112

113 Figure 1. Auditory brainstem response audiograms for the adult partially deafened  
 114 unstimulated (ADU) and adult deafened stimulated (ADS) animals at the time of the  
 115 acute electrophysiological experiment. Values are mean ( $\pm$  standard error of the mean).  
 116 Grey area indicates the 95% confidence range for normal-hearing animals (n=40 ears).

#### 117 2.4. Cochlear implantation and chronic stimulation

118 Approximately six months following deafening, eight partially deafened animals were  
 119 randomly selected and unilaterally implanted in the left cochlea with a Cochlear Ltd Hybrid  
 120 L14 cat electrode array (Shepherd et al., 2011), an extra-cochlear ball electrode in the  
 121 temporalis muscle, and lead-wire assembly, using previously published techniques (Coco et  
 122 al., 2007). Briefly, surgery was performed under aseptic conditions, with each animal  
 123 premedicated using atropine/acepromazine (ANAMAV, 0.05 ml/kg s.c.) and maintained at a  
 124 surgical level of anesthesia using a closed circuit anesthetic machine delivering a mixture of  
 125 isoflurane (1-3%) and oxygen. The array was inserted to approximately 50% the length of the  
 126 cat scala tympani, representing a tip electrode position of around 4 kHz (Irving et al., 2014).

127 Fourteen days after surgery, and every month thereafter during the chronic stimulation  
128 program, the cats were anesthetized with ketamine and xylazine (20 mg/kg i.m., 2 mg/kg s.c.)  
129 and an electrically evoked ABR (EABR) was recorded for each stimulating electrode. EABR-  
130 recording methods were as described previously (Fallon et al., 2009a). Approximately two  
131 weeks after the first EABR recordings the chronic stimulation program was initiated. Each  
132 animal received continuous unilateral stimulation at all available intra-cochlear electrodes  
133 from a Nucleus Freedom speech processor via a clinical stimulator (Cochlear Ltd, Sydney,  
134 Australia) situated within a custom-made backpack that was worn by the animal (Fallon et  
135 al., 2009a). The speech processors were programmed using standard clinical frequency  
136 allocation tables and delivered monopolar stimulation at 500 pulses per second (pps) per  
137 electrode. Each biphasic current pulse had a 25- $\mu$ s phase interval and an 8- $\mu$ s inter-phase gap,  
138 and stimulus level was varied from 3 dB below to 6 dB above the EABR threshold for that  
139 electrode. These adult-deaf stimulated (ADS group) cats were chronically stimulated for  
140 periods up to 8 months, with stimulation continuing until the commencement of the acute  
141 electrophysiological experiments. The acute experiments on the five adult-deafened  
142 unstimulated (ADU group) cats were carried out ~6months after deafening.

### 143 2.5. Cortical recording

144 Acute electrophysiological experiments to record surface LFPs from auditory cortex  
145 were performed at 38 – 93 weeks of age (see Table 1). Anesthesia was induced with ketamine  
146 and xylazine (20 mg/kg i.m., 2 mg/kg s.c.) and maintained at a steady, light level of surgical  
147 anesthesia via a slow intravenous infusion of sodium pentobarbitone (0.3 - 0.7 mg/kg/h). A  
148 tracheal cannula was inserted and respiration rate, end-tidal CO<sub>2</sub>, and core body temperature  
149 were maintained within normal levels (5-25 breaths/minute, 3-7% and 36-38 °C respectively).  
150 The ADU animals were acutely implanted (left ear) using the same surgical techniques and  
151 the same electrode arrays as used for the ADS animals.

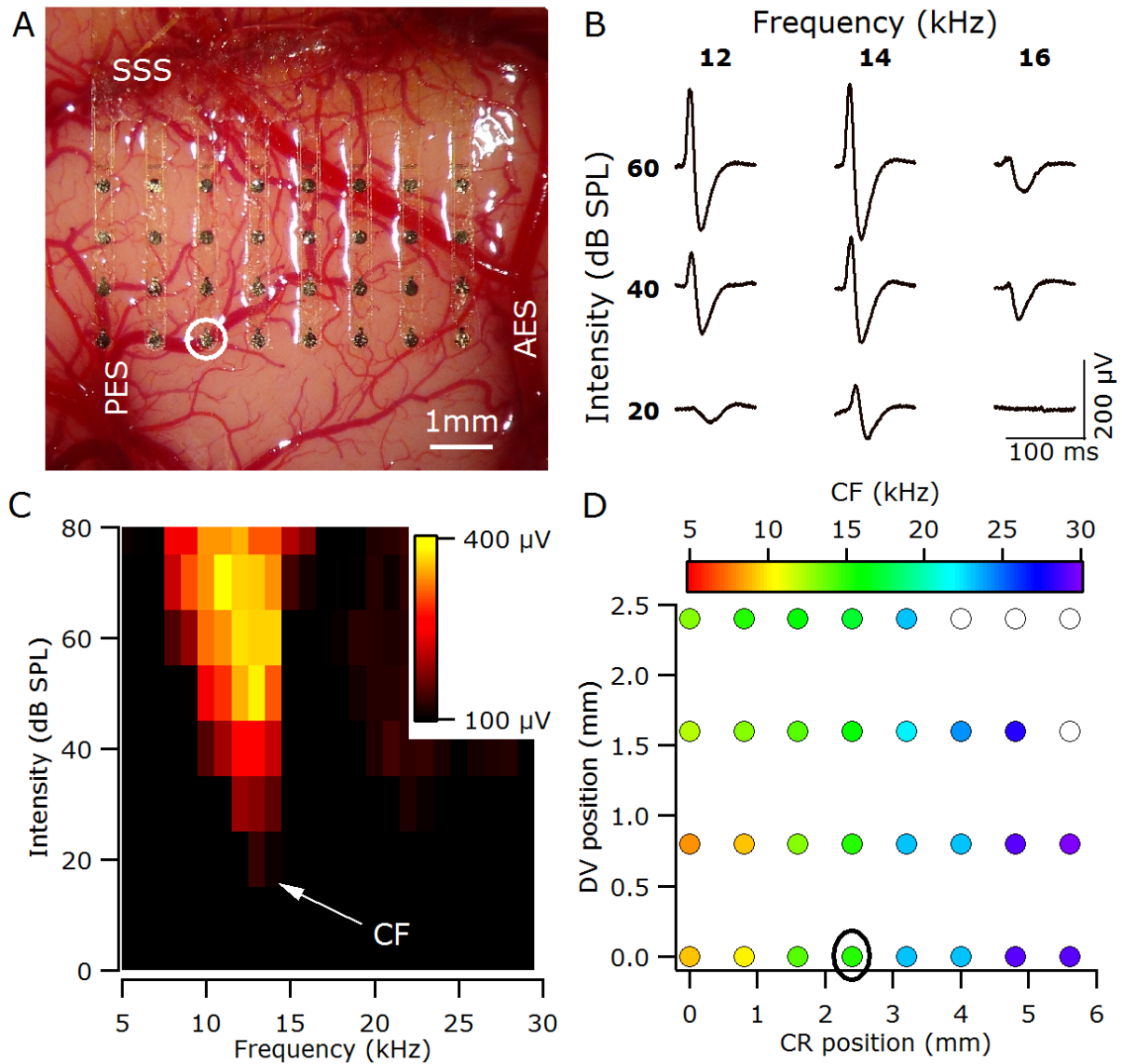
152           Animals were placed in a stereotaxic frame in an electrically shielded room, and a  
153 craniotomy was performed to expose the right auditory cortex. The thin-film surface array  
154 was placed over the middle ectosylvian gyrus (MEG), extending caudally from the anterior  
155 ectosylvian sulcus and ventrally from a position approximately 1 mm ventral of the  
156 suprasylvian sulcus (Figure 2A). Surface LFPs were captured at a sample rate of 10 kHz  
157 using the Cerebus system (Cyberkinetics; Foxborough, Massachusetts) and processed off-line  
158 in IgorPro (Wavemetrics; Lake Oswego, Oregon). Following LFP recordings, MU responses  
159 were recorded using standard techniques (Fallon et al., 2009b). Briefly, a 7x7 planar silicon  
160 array (Cyberkinetics; Foxborough, Massachusetts) was inserted in the middle of the MEG,  
161 and a linear array (A1x32-6mm-100-413-A32, NeuroNexus Technologies; Ann Arbor,  
162 Michigan) inserted down the rostral bank of the posterior ectosylvian sulcus. Recordings  
163 were captured at a sample rate of 30 kHz using the Cerebus system. At the end of the  
164 experiment the animals were terminated with an overdose of sodium pentobarbital (150  
165 mg/kg, intravenous).

## 166 *2.6. Acoustic stimulation and data analysis*

167           Acoustic stimuli were delivered via a calibrated 4" Vifa XT25TG30-04 speaker  
168 (Vifa, Videbæk, Denmark) driven by a TDT SA1 Stereo Power Amp (Tucker Davis  
169 Technologies, FL, USA). Stimuli consisted of 100-ms pure-tones (5-ms linear rise/fall)  
170 presented at 1 Hz at a range of frequency-intensity combinations (0.5 – 30 kHz in 1 kHz  
171 steps; 0 – 100 dB SPL in 5 dB steps). Each stimulus was presented 10 times with stimulus  
172 order randomized between repetitions.

173           For each recording site, the response area (RA) was determined by calculating the  
174 peak-to-peak amplitude of the LFP in the 100-ms window following the stimulus onset for  
175 each frequency-intensity combination (Figure 2B). These peak-to-peak values were then  
176 normalized to the maximum response to any stimulus for that recording site, and used to  
177 determine the threshold (the lowest sound pressure level at which the peak-to-peak amplitude

178 was significantly (more than 2 standard deviations) above the background noise level) and  
 179 characteristic frequency (CF, frequency with the lowest threshold) for that recording site  
 180 (Figure 2C). In this way the tonotopic organisation for the area under the entire recording  
 181 array could be determined (Figure 2D).



182

183 Figure 2. (A) The thin-film recording array covers the majority of the right primary  
 184 auditory cortex in a normal-hearing animal (6\_19). SSS, suprasylvian sulcus; AES,  
 185 anterior ectosylvian sulcus; PES, posterior ectosylvian sulcus. (B) Sample local field  
 186 potentials (LFPs) recorded from the location circled in A & D. LFPs are the averaged  
 187 response to 10 stimuli, with the first 100 ms of the response shown. (C) Response area,  
 188 plots the peak-to-peak amplitude of the LFP (yellow-maximum, black minimum) for the  
 189 recording site circled in A & D. The CF for this site was 14 kHz. (D) Tonotopic  
 190 organisation of auditory cortex determined using analysis of response areas based on

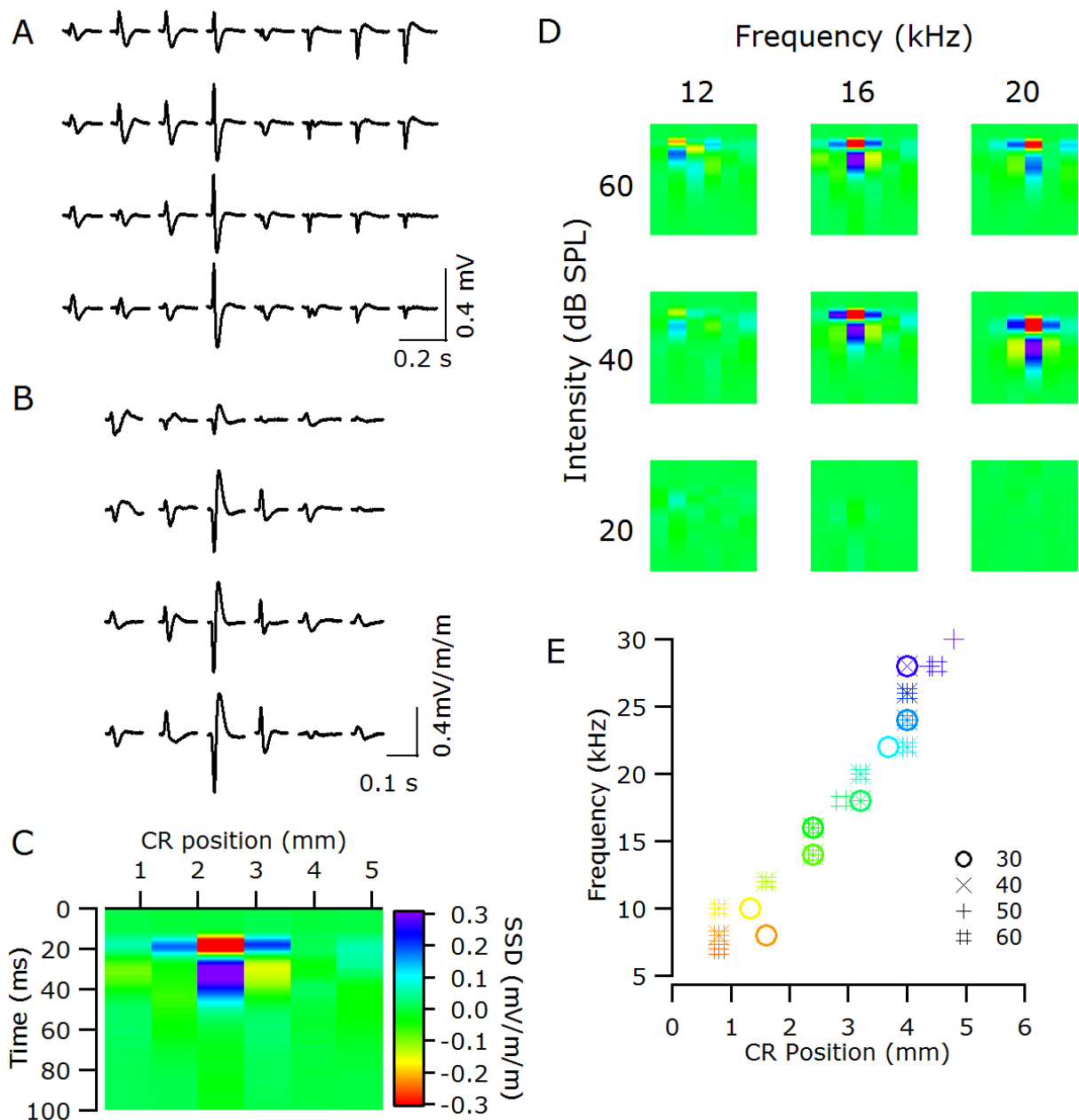
191 LFPs. Filled symbols represent the characteristic frequency (CF) at each recording site.  
192 Open symbols indicate recordings sites for which it was not possible to determine a CF;  
193 CR, caudal-rostral position relative to electrode closest to the tip of PES; DV, dorsal-  
194 ventral position relative to electrode closest to the tip of PES.

195 Additionally, a new analysis based on the second spatial derivative was used to  
196 determine the tonotopic organisation. The 32-channel rectangular array was analysed as four  
197 separate 8-channel caudal-rostral linear electrode arrays (Figure 3A). For each frequency-  
198 intensity combination, the SSD was computed at each sampled time-point from 0 to 100ms  
199 post stimulus onset (Figure 3B) according to the formula:

$$SSD_t^d = \frac{\phi_t^{r-\Delta r} - 2 \times \phi_t^r + \phi_t^{r+\Delta r}}{\Delta r^2}$$

200 where  $\phi_t^r$  represents the potential amplitudes recorded at caudal-rostral location r with  
201 latency t.

202 For a supra-threshold stimulus, the SSD analysis produced a stereotypical pattern of a  
203 single negative maximum (e.g., red area in Figure 3C) flanked in the caudal and rostral  
204 directions by positive maxima (e.g., dark blue areas at 20ms in Figure 3C). For each  
205 frequency – intensity combination, the location along the caudal-rostral axis at which the  
206 largest negative maximum occurred was used in plots of frequency against caudal-rostral  
207 position (Figure 3E) to determine the tonotopic organization.



208  
209

210 Figure 3. (A) Sample local field potentials (LFPs) recorded to a 60 dB SPL 16 kHz tone  
 211 across the thin-film array in a normal-hearing animal (6\_19). (B) The second spatial  
 212 derivative (SSD) of the LFPs evoked by that stimulus. (C) The bottom row of the array  
 213 exhibits a single negative maximum at 2.4 mm rostral of the tip of the posterior  
 214 ectosylvian sulcus, which is flanked in the caudal and rostral directions by positive  
 215 maxima. The positioning of the SSD is relative to the responses illustrated in A & B. (D)  
 216 Sample SSDs from the bottom row of the array in response to different frequency-  
 217 intensity combinations (same conventions as C). (E) Tonotopic organization of auditory  
 218 cortex in 6\_19 determined using SSD analysis. Different symbols represent analysis at  
 219 different dB SPLs; color scale matches Figure 2D. CR, caudal-rostral position relative to  
 220 electrode closest to the tip of the posterior ectosylvian sulcus.

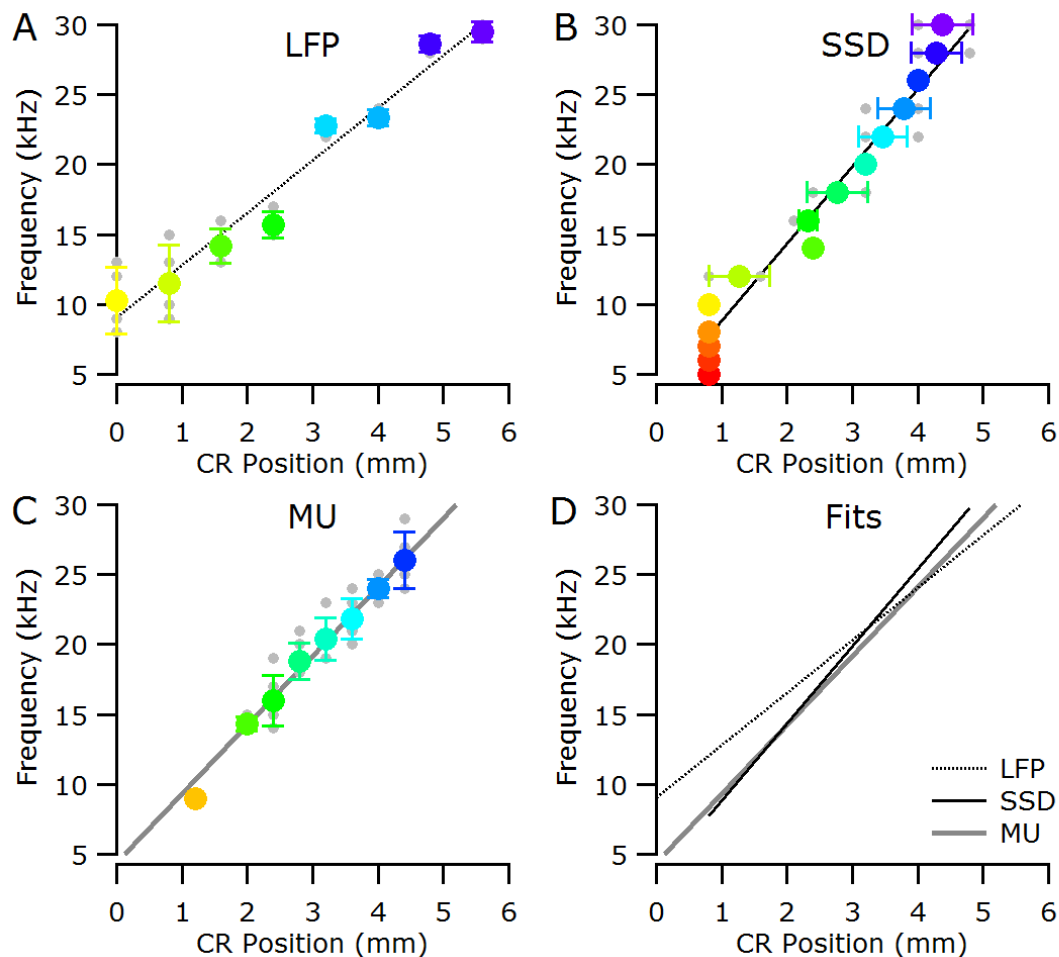
221 Finally, MU activity was analyzed using standard techniques (Fallon et al., 2009a).  
222 Briefly, MU RAs were determined from the number of threshold (set to -4 times the root-  
223 mean-squared background) crossings in the 5 – 55 ms following stimulus onset. These spike  
224 counts were then normalized to the maximum response to any stimulus for that recording site,  
225 and used to determine the threshold (normalised response significantly above the background  
226 level) and CF.

### 227 **3. Results**

228 Tone-evoked LFPs could be recorded from all fourteen animals. The LFPs from the  
229 normal-hearing animal (6-19) will be used to demonstrate several features of the SSD  
230 analysis, and provide an initial validation of this analysis by comparison with MU data.  
231 Additional validation will be provided by a comparison of LFP, SSD and MU data from the  
232 ADS and ADU animals concerning the effects of partial deafness and cochlear electrical  
233 stimulation on acoustic responsiveness.

234 As illustrated in Figure 2C, the CF for a given recording site is defined as the  
235 frequency with the lowest threshold; therefore, the tonotopic organisation observed using CF  
236 (Figure 2D) is defined only at threshold levels. At supra-threshold stimulus levels the best  
237 frequency (BF; the frequency eliciting the largest response at a particular sound pressure  
238 level) is sometimes used, and as is clear from Figure 2C, the BF can change with stimulation  
239 level (the maximum response shifts to lower frequencies with increasing level in Figure 2C  
240 and is 11kHz at 70 dB SPL). In contrast, with SSD analysis of the LFPs the location of the  
241 central negative maximum is relatively insensitive to level, provided the stimulus is supra-  
242 threshold (Figure 3D). The overlap of the different symbols, representing different stimulus  
243 intensities, in Figure 3E highlights this level invariance of the central negative maximum for  
244 a given stimulus frequency. The location of the central negative maximum does, however,  
245 shift with stimulus frequency (Figure 3E and Figure 4B, Pearson correlation;  $P < 0.001$ ) and  
246 exhibits the expected caudal-rostral shift with increasing stimulus frequency). Plots of CF  
247 against caudo-rostral position for the LFP and MU data are shown Figure 4A and C

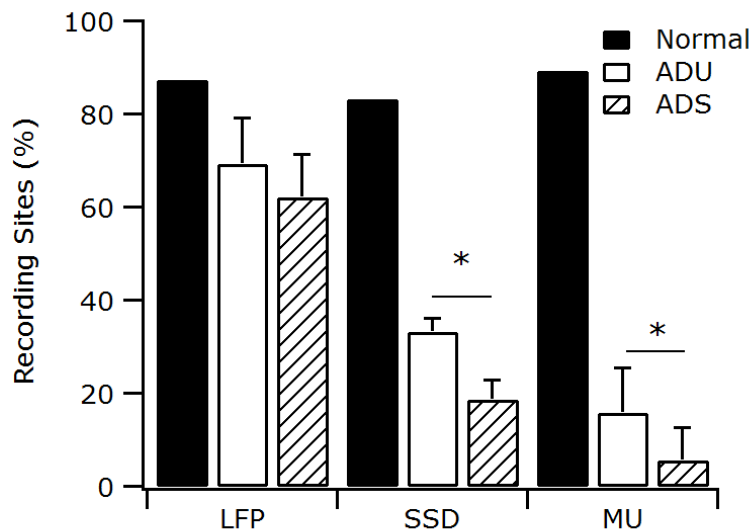
248 respectively, and the linear fits for three analyses are plotted together in Figure 4D. The slope  
 249 of the SSD function (5.5 kHz / mm) is similar to that computed from the MU CFs (4.9 kHz /  
 250 mm), and both are substantially higher than that computed from the LFP CFs (3.8 kHz / mm),  
 251 consistent with the finding that CF gradients determined from LFPs underestimate the true  
 252 gradient (Eggermont et al., 2011).



253

254 Figure 4. Data from a normal-hearing cat (6\_19). (A) Characteristic frequency (CF) as  
 255 determined from the LFP response areas plotted against caudal-rostral position. (B)  
 256 Location of the negative maximum in the SSD analysis for a given stimulus frequency.  
 257 (C) CF as determined from the multi-unit (MU) activity plotted against caudal-rostral  
 258 position. In all panels, individual data points are shown in grey; colored symbols are  
 259 mean ( $\pm$  standard deviation). Lines represent fits to the caudal-rostral shift with  
 260 increasing stimulus frequency. (D) Overlay of the linear fits for LFP, SSD and MU  
 261 analysis. CR, caudal-rostral position relative to electrode closest to the tip of the posterior  
 262 ectosylvian sulcus.

263           In Figure 5, the proportions of recording sites to which frequencies could be assigned  
264 using LFP, SSD and MU analyses are shown for the normal-hearing cat and the two groups  
265 of partially deafened cats. For the normal-hearing cat, the proportions are similar (in the  
266 range 80-90%) for the three methods. In the LFP analysis, the proportion of locations to  
267 which a CF could be assigned was reduced by approximately 20% in the partially deafened  
268 cats, to  $69.3\% \pm 9.7\%$  and  $62.1\% \pm 9.1\%$  (mean  $\pm$  standard error of the mean) sites in the  
269 ADU and ADS animals, respectively. This difference between the two partially deafened  
270 groups was not significant (t-Test,  $t = 0.5466$ ,  $p = 0.597$ ). In contrast, the proportion of sites  
271 that were assigned a frequency by the SSD analysis was substantially reduced (by 50% or  
272 more) in the partially deafened animals: only  $33.3\% \pm 2.9\%$  and  $18.8\% \pm 4.2\%$  mean  $\pm$   
273 standard error of the mean) of the recording sites in the ADU and ADS groups, respectively,  
274 exhibited a local minimum. In contrast to the LFP analysis, this difference between the  
275 groups was significant (t-Test,  $t = 2.824$ ,  $p = 0.017$ ). Finally, the proportion of locations to  
276 which a CF could be assigned with the MU analysis was even further reduced; only  $15.9\% \pm$   
277  $9.5\%$  and  $5.7\% \pm 6.9\%$  mean  $\pm$  standard error of the mean) of the recording sites in the ADU  
278 and ADS groups, respectively. As with the SSD analysis, this difference was significant (t-  
279 Test,  $t=1.950$ ,  $p = 0.0399$ ). Both the SSD and MU analyses therefore differ from the LFP  
280 analysis in showing a substantial reduction of responsive sites in the partially deafened  
281 animals and a significant difference between the ADU and ADS groups.



282

283 Figure 5. Proportion of recording sites to which frequencies could be assigned for the  
 284 three groups of animals using standard local field potential response area analysis (LFP),  
 285 SSD analysis and multi-unit (MU) activity. There was a significant difference between  
 286 the adult deafened unstimulated (ADU) and adult deafened stimulated (ADS) groups (\*,  
 287  $p < 0.05$ ) using the both the SSD and MU analyses but not the standard LFP analysis.

## 288 4. Discussion

289 The use of a thin-film polyimide substrate electrode array to record surface LFPs  
 290 provides several advantages over sequential recordings made with either macro- or micro-  
 291 electrodes. The greatest advantage is the ability to record simultaneously from large cortical  
 292 regions, which eliminates possible confounds with changes in cortical responsiveness over  
 293 time. The reduction in recording time is a further advantage, as it potentially allows more  
 294 data to be obtained within a given experiment. The ability of the flexible electrode array,  
 295 combined with the specific geometry of the fingers of electrodes, to conform to surface  
 296 topology, also results in more consistent recording conditions. Furthermore, simultaneous  
 297 recording from multiple sites allows the use of SSD analysis of the surface LFPs. Finally, the  
 298 less invasive nature of the surface electrode, compared to MU recording electrodes, would be  
 299 expected to results in improved long-term performance during chronic implantation.

300 The tonotopic organization of the primary auditory cortex on the cat's MEG was  
 301 originally established using LFP recordings (Woolsey & Walzl, 1942) and has been described

302 in detail using MU recordings (Aitkin, 1990; Merzenich et al., 1975; Reale & Imig, 1980).  
303 The frequency-to-cortex mapping using MU recordings in the normal-hearing cat in the  
304 current study was 4.9 kHz / mm, within the range of  $5.3 \pm 0.3$  kHz / mm we have previously  
305 reported using MU recordings from penetrating microelectrodes in normal-hearing cats  
306 (Fallon et al., 2009a). The value of 5.5 kHz / mm obtained with SSD analysis also falls within  
307 this normal MU data range. In contrast, the mapping using LFP analysis was 3.0 kHz / mm.  
308 This shallower mapping is consistent with the broader spreading of LFPs resulting in  
309 underestimation of the gradient as determined with spiking activity (Eggermont et al., 2011).  
310 The effective increase in the spatial resolution obtained with SSD analysis of the LFPs brings  
311 it within the range achievable with more invasive single-unit or MU recording, and  
312 constitutes a significant advantage of this technique.

313         The improved spatial resolution of the SSD analysis also allowed us to observe a  
314 significant reduction in the proportion of acoustically responsive sites in the MEG of partially  
315 deafened cats following chronic intra-cochlear stimulation. This finding is consistent with our  
316 previous report using standard electrophysiology and penetrating microelectrodes in  
317 neonatally ototoxically partially deafened animals (Fallon et al., 2009b). The proportions in  
318 our previous study (82% and 58% for unstimulated and stimulated groups respectively) are  
319 much higher than those in the present study, reflecting the fact that recordings in that study  
320 were made with single microelectrodes. The ability to move the electrode throughout the  
321 depth of the cortex in the search for driven activity greatly increases the possibility of being  
322 able to determine a CF. The important point, however, is that the SSD analysis revealed a  
323 difference that has been seen consistently in MU activity but was not apparent using the  
324 standard CF analysis of the LFPs. As noted above, volume conduction spatially smears the  
325 LFPs, and this smearing is ameliorated by the improved spatial resolution provided by the  
326 SSD analysis.

327           The data we have presented establish that the SSD analysis provides descriptions of  
328 normal AI tonotopy, and of responsiveness in partially deafened animals, that are much more  
329 similar to those provided by MU data than are descriptions based on LFP analysis. A feature  
330 not captured by the SSD analysis is the change in BF that can occur with stimulation level  
331 with both MU and LFP analysis (see Figure 2C). In fact, SSD analysis is relatively  
332 insensitive to level, provided the stimulus is supra-threshold (see Figure 3D). The reasons for  
333 this level-invariance of assigned frequency with the SSD method are unclear, but would not  
334 seem to offset its advantages unless the issue under consideration were the effects of level on  
335 frequency selectivity.

336           The current thin-film polyimide substrate electrode array has been specifically  
337 designed for AI in the cat, although it could be easily adapted to other cortical areas (e.g.  
338 primary visual cortex) or other species. Design modifications for different sized cortical areas  
339 would need to trade-off the number of electrodes and the center-to-center spacing. The  
340 current design utilizes 800  $\mu\text{m}$  center-to-center spacing as the LFP signal drops by ~50% in  
341 400  $\mu\text{m}$  (Cottaris & Elfar, 2009), but the spacing could be adjusted as required. As the  
342 exposed electrode materials of platinum and polyimide are biological compatible, the use of  
343 the thin-film polyimide substrate electrode array and SSD analysis could provide a viable  
344 method of chronically monitoring cortical plasticity in humans, without the injury concerns  
345 of using penetrating electrode arrays (Jorfi et al., 2015). Finally, the SSD analysis may prove  
346 useful in the analysis of other surface recordings such as epilepsy monitoring and brain  
347 machine interfaces.

## 348 **5. Acknowledgments**

349           This work was funded by the NH&MRC (GNT1002430) and National Institute of  
350 Deafness and Other Communication Disorders (NIH Y1-DC-8002-01) and Lawrence  
351 Livermore National Laboratory. The Bionics Institute acknowledges the support it receives  
352 from the Victorian Government through its Operational Infrastructure Support Program.

353            We thank Vanessa Tolosa, Kedar Shah, Sarah Felix and Nicole Critch for technical  
354 assistance.  
355

## 356 6. References

- 357 Aitkin, L. 1990. *The Auditory Cortex. Structural and Functional Bases of Auditory*  
358 *Perception* Chapman and Hall, London, UK.
- 359 Coco, A., Epp, S.B., Fallon, J.B., Xu, J., Millard, R.E., Shepherd, R.K. 2007. Does cochlear  
360 implantation and electrical stimulation affect residual hair cells and spiral ganglion  
361 neurons? *Hear Res* 225, 60-70.
- 362 Cottaris, N., Elfar, S. 2009. Assessing the efficacy of visual prostheses by decoding ms-LFPs:  
363 application to retinal implants. *J Neural Eng* 6, 026007.
- 364 Eggermont, J.J., Munguia, R., Pienkowski, M., Shaw, G. 2011. Comparison of LFP-based  
365 and spike-based spectro-temporal receptive fields and cross-correlation in cat primary  
366 auditory cortex. *PLoS One* 6, e20046.
- 367 Fallon, J.B., Irvine, D.R.F., Shepherd, R.K. 2009a. Cochlear implant use following neonatal  
368 deafness influences the cochleotopic organization of the primary auditory cortex in  
369 cats. *J Comp Neurol* 512, 101-114.
- 370 Fallon, J.B., Shepherd, R.K., Brown, M., Irvine, D.R. 2009b. Effects of neonatal partial  
371 deafness and chronic intracochlear electrical stimulation on auditory and electrical  
372 response characteristics in primary auditory cortex. *Hear Res* 257, 93-105.
- 373 Gaucher, Q., Edeline, J.M., Gourevitch, B. 2012. How different are the local field potentials  
374 and spiking activities? Insights from multi-electrodes arrays. *Journal of physiology,*  
375 *Paris* 106, 93-103.
- 376 Irving, S., Wise, A.K., Millard, R.E., Shepherd, R.K., Fallon, J.B. 2014. A partial hearing  
377 animal model for chronic electro-acoustic stimulation. *J Neural Eng* 11, 046008.
- 378 Jorfi, M., Skousen, J.L., Weder, C., Capadona, J.R. 2015. Progress towards biocompatible  
379 intracortical microelectrodes for neural interfacing applications. *J Neural Eng* 12,  
380 011001.
- 381 Kajikawa, Y., Schroeder, C.E. 2011. How local is the local field potential? *Neuron* 72, 847-  
382 58.
- 383 Klinke, R., Kral, A., Heid, S., Tillein, J., Hartmann, R. 1999. Recruitment of the auditory  
384 cortex in congenitally deaf cats by long-term cochlear electrostimulation. *Science*  
385 285, 1729-33.
- 386 Kral, A., Tillein, J., Heid, S., Hartmann, R., Klinke, R. 2005. Postnatal cortical development  
387 in congenital auditory deprivation. *Cereb Cortex* 15, 552-62.
- 388 Kral, A., Tillein, J., Hubka, P., Schiemann, D., Heid, S., Hartmann, R., Engel, A.K. 2009.  
389 Spatiotemporal patterns of cortical activity with bilateral cochlear implants in  
390 congenital deafness. *J Neurosci* 29, 811-27.
- 391 Merzenich, M.M., Knight, P.L., Roth, G.L. 1975. Representation of cochlea within primary  
392 auditory cortex in the cat. *J Neurophysiol* 38, 231-49.
- 393 Middlebrooks, J.C. 2008. Auditory cortex phase locking to amplitude-modulated cochlear  
394 implant pulse trains. *J Neurophysiol* 100, 76-91.
- 395 Mitzdorf, U. 1985. Current source-density method and application in cat cerebral cortex:  
396 investigation of evoked potentials and EEG phenomena. *Physiological Reviews* 65,  
397 37-100.
- 398 Müller-Preuss, P., Mitzdorf, U. 1984. Functional anatomy of the inferior colliculus and the  
399 auditory cortex: current source density analyses of click-evoked potentials. *Hear Res*  
400 16, 133-142.
- 401 Norena, A., Eggermont, J.J. 2002. Comparison between local field potentials and unit cluster  
402 activity in primary auditory cortex and anterior auditory field in the cat. *Hear Res* 166,  
403 202-13.
- 404 Reale, R.A., Imig, T.J. 1980. Tonotopic organization in auditory cortex of the cat. *J Comp*  
405 *Neurol* 192, 265-91.

- 406 Schroeder, C.E., Lindsley, R.W., Specht, C., Marcovici, A., Smiley, J.F., Javitt, D.C. 2001.  
407 Somatosensory input to auditory association cortex in the macaque monkey. *J*  
408 *Neurophysiol* 85, 1322-1327.
- 409 Shepherd, R., Verhoeven, K., Xu, J., Risi, F., Fallon, J., Wise, A. 2011. An improved  
410 cochlear implant electrode array for use in experimental studies. *Hear Res* 277, 20-27.
- 411 Tooker, A., Tolosa, V., Shah, K.G., Sheth, H., Felix, S., Delima, T., Pannu, S. 2012.  
412 Optimization of multi-layer metal neural probe design, *Engineering in Medicine and*  
413 *Biology Society (EMBC), 2012 Annual International Conference of the IEEE. IEEE.*  
414 pp. 5995-5998.
- 415 Woolsey, C.N., Walzl, E.M. 1942. Topical projection of nerve fibers from local regions of  
416 the cochlea to the cerebral cortex. *Bulletin of Johns Hopkins Hospital* 71, 315-344.  
417  
418

419 **Table 1. Details of deafening and stimulation times for individual animals**

Group	Animal ID	Deafening (weeks)	Chronic Stimulation (weeks)	Age (weeks)
Normal-Hearing Control (NHC)	6_19	-	-	38
Adult deafened unstimulated (ADU)	6_23	44	-	73
	6_24	45	-	69
	6_25	35	-	58
	6_27	45	-	74
	6_28	32	-	59
Adult deafened stimulated (ADS)	6_02	31	68	88
	6_11	34	66	93
	6_12	34	66	91
	6_13	34	66	92
	6_14	35	69	91
	6_15	35	70	93
	6_16	35	69	88
	6_17	36	70	88

420 Individual animals in the experimental groups are specified by identification (ID)  
 421 number; Deafening is the age at the initiation of deafening injections; Chronic  
 422 Stimulation is the age at the beginning of the ICES regime which continued until the  
 423 acute experiment; Age is the age at the time of the acute experiment.